RMP Colloquia

This section, offered as an experiment beginning in January 1992, contains short articles intended to describe recent research of interest to a broad audience of physicsts. It will concentrate on research at the frontiers of physics, especially on concepts able to link many different subfields of physics. Responsibility for its contents and readability rests with the Advisory Committee on Colloquia, U. Fano, chair, Robert Cahn, S. Freedman, P. Parker, C. J. Pethick, and D. L. Stein. Prospective authors are encouraged to communicate with Professor Fano or one of the members of this committee.

Electron-scattering studies of correlations in nuclei

O. Benhar* and V. R. Pandharipande

Department of Physics, University of Illinois, Urbana, Illinois 61801-3080

Steven C. Pieper

Physics Division, Argonne National Laboratory, Argonne, Illinois 60439-4843

The authors review theoretical estimates of spatial, spin, and isospin correlations among the nucleons in nuclei. The momentum distribution and spectral function of nucleons in nuclei are also discussed. The theoretical estimates are compared with the observed correlation effects in the inclusive scattering of electrons from nuclei, at energies ranging from a few hundred MeV to several GeV. The observed transparencies of nuclei to protons ejected in inclusive $e,e'p$ reactions are also compared with their theoretical estimates. Finally, the quenching of exclusive single-quasiparticle-type reactions, indicative of the overall strength of correlations in nuclei, is discussed. There appears to be a qualitative agreement between theory and experiment, but a firm quantitative understanding is still to be obtained.

CONTENTS

I. INTRODUCTION

Interparticle forces induce correlations among the constituents of a many-body system. Atomic liquid ^{4}He, whose atoms are kept apart by the strong repulsive core in the interatomic potential, and whose correlations have been analyzed successfully by neutron scattering, is viewed here as a prototype. The probability of finding two atoms simultaneously at $\mathbf{r}_1$ and $\mathbf{r}_2$ is expressed as $\rho^2 g(r_{12})$, where ρ is the density of the liquid, $g(r)$ is the *pair distribution function,* and $\mathbf{r}_{12}=\mathbf{r}_1-\mathbf{r}_2$. The $g(r)$ equals 1 in the absence of any correlations, but in liquid ^{4}He it is essentially zero at small r, as shown in Fig. 1. The $g(r)$ is determined by the interatomic potential $v(r)$, also shown in Fig. 1, and by the density of the liquid. The Fourier transform of $g(r)$ determines the liquid *structure function*:

$$S(q)=1+\rho g(q)\ , \tag{1.1}$$

which has been measured for liquid ^{4}He by neutron (Svensson *et al.*, 1980) and x-ray (Hallock, 1972) scattering. The function $g(r)$ has been calculated with the Green's-function Monte Carlo (GFMC) method by Kalos *et al.* (1981) using realistic models of $v(r)$ obtained by Aziz *et al.* (1979), yielding close agreement between theory and experiment. Correlations generate high-momentum components in the wave functions of liquids, whose effect on the neutron scattering has been studied. The $g(r)$ and the momentum distribution of atoms in the Fermi-liquid ^{3}He have also been studied experimentally as well as theoretically. A book edited by Silver and Sokol (1989) contains recent reviews on the momentum distribution of atoms in helium liquids and their measurement by neutron-scattering experiments.

This colloquium reviews the more difficult problem of studying the correlations among nucleons in atomic nuclei, specifically for small nuclei up to ^{16}O and for nuclear matter (NM). The nucleon-nucleon (NN) interaction has a strong dependence on the spins and charges of the interacting pair. The nucleon charge has only two values, 1 for proton and zero for neutron; it is represented by an *isotopic spin* variable $\vec{\tau}$ similar to the spin operator $\vec{\sigma}$. All nucleons are considered as identical fermions with four possible spin-isospin states. Nuclear forces induce both spatial and spin-isospin correlations, which are influenced by the size of the nucleus. The theoretical predictions of correlations in nuclei are reviewed in Sec. II. Sections II.A and II.B describe models of nuclear forces and the ground states of nuclei, while the pair and momentum distribution functions of nucleons in nuclei are discussed in Secs. II.C and II.D.

The spectral function $P_h(\mathbf{k},e)$ describes the probability of a nucleon in the nucleus having momentum $\mathbf{k}$ and en-

*Present address: The Istituto Nazionale di Física Nucleare, Sezione Sanitá, I-00161 Rome, Italy.

 0034-6861/93/65(3)/817(12)/$06.20

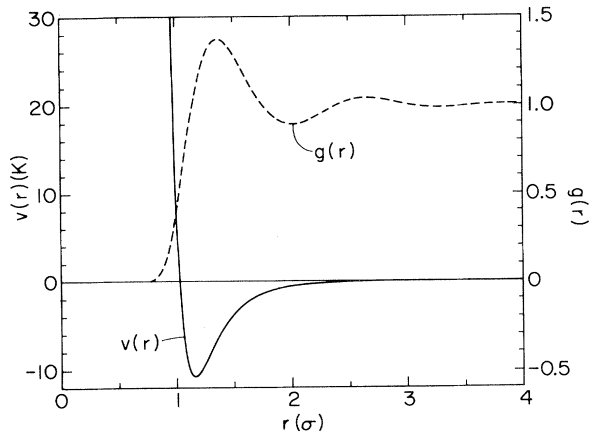

FIG. 1. The $v(r)$ of Aziz *et al.* (1979) shown by the solid line and left scale, and the $g(r)$, calculated by Kalos *et al.* (1981), in liquid ^{4}He at equilibrium density, shown by the dashed line and the right scale.

ergy e. High-energy ($>$ GeV) electrons essentially see the nucleus as a collection of nucleons distributed according to $P_h(\mathbf{k},e)$. Thus the spectral functions are useful in the study of electron-nucleus scattering, and correlation effects in the $P_h(\mathbf{k},e)$ are discussed in Sec. II.E.

In the qualitatively successful simple shell model of nuclei, the nucleons in a nucleus move in the single-particle orbitals of an average potential. Some aspects of this simple picture are valid even when there are significant correlations between the nucleons. The single-particle or hole states of the shell model have to be reinterpreted as quasiparticle states, and there is an associated probability Z, called the quasiparticle normalization constant, with which the quasiparticle acts as a single particle. Several electron-scattering experiments are sensitive to the value of Z, whose theoretical estimates are discussed in Sec. II.E

Nuclear correlations are experimentally studied by observing the scattering of electrons by nuclei, but this task is more difficult than the corresponding studies of helium liquids by neutron scattering. The kinetic energy of atoms in helium liquids is of order 10 K (10^{-3} eV), and neutrons with energies of order 1000 K (0.1 eV) are typically used. The first excited state of the helium atom has a much larger energy (20 eV); hence helium atoms appear inert to the neutron. In contrast, the kinetic energies of nucleons in nuclei are of order 30 MeV, and the first excited state of the nucleon, the Δ resonance, has an excitation energy of only $\sim$300 MeV. Effects of internal excitations of the nucleons have thus to be considered in the analysis of high-energy (typically 0.5 to 10 GeV) electron scattering by nuclei; relativistic effects are often not negligible. In addition to the "inclusive" scattering experiments, in which the final state of the nucleus is not observed, scattering to specific final states is also studied. In contrast, only inclusive neutron-scattering experiments have been performed on helium liquids.

Results of selected electron-nucleus scattering experiments are reviewed in Sec. III, and we end with a brief summary presented in Sec. IV.

II. THEORETICAL ESTIMATES OF CORRELATIONS IN NUCLEI

A. Models of nuclear forces

The nonrelativistic nuclear many-body theory, based on the Hamiltonian

$$H=-\frac{\hbar^2}{2m}\sum_i \nabla_i^2+\sum_{i<j} v(ij)+\sum_{i<j<k} V(ijk)\ , \quad (2.1)$$

has served extensively in studies of nuclear ground states (Pandharipande, 1990; Wiringa, 1993). The long-range part of $v(ij)$ consists of the one-pion-exchange potential $v^\pi(ij)$:

$$v^\pi(ij)=\frac{1}{3}\frac{f^2}{4\pi}\mu X_{ij}\tau_i\cdot\tau_j\ , \quad (2.2)$$

$$X_{ij}(r_{ij}\to\infty)=\left[\sigma_i\cdot\sigma_j+\left[1+\frac{3}{\mu r_{ij}}+\frac{3}{\mu^2 r_{ij}^2}\right]S_{ij}\right]\frac{e^{-\mu r_{ij}}}{\mu r_{ij}}\ . \quad (2.3)$$

f and μ are the pion-nucleon coupling constant and pion mass; σ_i and τ_i are nucleon spin and isospin operators; and S_{ij} is the tensor operator:

$$S_{ij}=3\sigma_i\cdot\hat{r}_{ij}\sigma_j\cdot\hat{r}_{ij}-\sigma_i\cdot\sigma_j\ . \quad (2.4)$$

The operator $v^\pi(ij)$ is dominated by its tensor part, and its short-range singular part needs to be regularized, since nucleons are finite-size bound states of quarks. An accurate determination of f^2, with $<1\%$ error, has been made recently by Stoks, Timmermans, and de Swart (1992); however, most models of $v(ij)$ use older values of f^2, which are up to 8% larger.

The long-range part of the three-nucleon interaction $V(ijk)$ consists of the two-pion-exchange interaction $V^{2\pi}(ijk)$,

$$V^{2\pi}(ijk)=\sum_{\text{cyc}} A_{2\pi}(\{X_{ij},X_{jk}\}\{\tau_i\cdot\tau_j,\tau_j\cdot\tau_k\}+\tfrac{1}{4}[X_{ij},X_{jk}][\tau_i\cdot\tau_j,\tau_j\cdot\tau_k])\ , \quad (2.5)$$

summed over three terms obtained by cyclic permutations of i, j, and k. Its strength $A_{2\pi}$ is not uniquely known (Gibson and McKellar, 1988). The rest of the interactions, $v^R(ij)$ and $V^R(ijk)$, are not yet well understood. Detailed phenomenological models of $v^R(ij)$ have been obtained by fitting the significant amount of available NN scattering data. We shall discuss results obtained with the "Urbana" (Lagaris and Pandharipande, 1981) and "Argonne" (Wiringa, Smith, and Ainsworth, 1984) models of $v(ij)$; other models are also in use. These models indicate that the $v^R(ij)$ has a strong repulsive core and an intermediate-range attraction independent of spin and isospin. These components are often attributed to effective vector and scalar meson-exchange interactions. The $v^R(ij)$ also has important components dependent on spin orbit, spin-isospin, and momentum. A simple $V^R(ijk)$ of strength U_0, independent of spin-

isospin, is assumed in the Urbana models of $V(ijk)$ [Schiavilla, Pandharipande, and Wiringa (1986)]. At present rather few observables can be calculated accurately with the Hamiltonian (2.1), limiting us to simple models of $V(ijk)$ with only two parameters, $A_{2\pi}$ and U_0.

B. Nuclear ground states

The ground states of ^{3}H and ^{3}He have been calculated essentially exactly with Faddeev's method (Friar, 1991); almost exact calculations have also been performed for nuclei with $A \leq 5$ with the GFMC method (Carlson, 1991). Exact calculations for $A > 8$ seem to be impractical with the presently available methods and foreseeable computers. The variational method (Wiringa, Fiks, and Fabrocini, 1988; Wiringa, 1991; Pieper, Wiringa, and Pandharipande, 1992) has been used to study ^{2}H, ^{3}H, ^{3}He, ^{4}He, ^{16}O, ^{40}Ca, and nuclear matter (NM) in a unified way with variational wave functions of the form

$$\Psi_v = \left[\prod_{\rm IT}(1+U_3(ijk))\right]\left[S\prod_{i<j}(1+U(ij))\right] \times\left[\prod_{i<j} f_c(r_{ij})\right]\Phi\ , \tag{2.6}$$

where $U_3(ijk)$ represent three-nucleon correlation operators with the same spin-isospin structure as $V(ijk)$, and the label IT (independent triplets) restricts the products of U_3's, in the expansion of $\Pi\,(1+U_3)$ in powers of U_3, to those having independent triplets ijk, lmn, ... This restriction avoids treating the nonvanishing commutators $[U_3(ijk), U_3(ilm)]$ of these less important correlations. The $U(ij)$ consist of two-body correlation operators:

$$U(ij)=u_\sigma(r_{ij})\sigma_i\cdot\sigma_j+u_t(r_{ij})S_{ij}+u_{LS}(r_{ij})\mathbf{L}\cdot\mathbf{S} +[u_\tau(r_{ij})+u_{\sigma\tau}(r_{ij})\sigma_i\cdot\sigma_j+u_{t\tau}(r_{ij})S_{ij} +u_{LS\tau}(r_{ij})\mathbf{L}\cdot\mathbf{S}]\tau_i\cdot\tau_j\ . \tag{2.7}$$

The sum-product notation $S\prod$ in Eq. (2.6) denotes a symmetrized product of the noncommuting operators $U(ij), U(ik)\ldots$. The function $f_c(r_{ij})$ in Eq. (2.6) represents central, spatial correlations induced mostly by the repulsive core in $v^R(ij)$, and Φ stands for an antisymmetric product of single-particle states. In the case of NM, Φ indicates the Fermi-gas wave function, while in ^{16}O and ^{40}Ca it represents a Slater determinant appropriate to the shell model. In these systems we assume the limiting values $f_c\ (r_{ij}\to\infty)=1$, and $U(r_{ij}\to\infty)=0$. In contrast, for ^{2}H, ^{3}H, ^{3}He, and ^{4}He, Φ represents a spin-isospin state with no spatial dependence, and $f_c\ (r_{ij}\to\infty)$ must vanish for bound states. The calculations for finite nuclei are more advanced; they utilize Monte Carlo methods to evaluate expectation values with the complete Ψ_V described above. The presently available NM calculations rely on chain summation methods and on a Ψ_v shorn of three-body correlations; the relatively poor quality of the NM Ψ_v is partly compensated by calculating corrections to variational results derived by correlated basis perturbation theory (Fantoni, Friman, and Pandharipande, 1983).

TABLE I. Results of variational calculations with Argonne $v(ij)$ and Urbana model VII $V(ijk)$ in MeV.

	^{2}H	^{3}He	^{4}He	^{16}O	NM
(E_0/A) Expt.	−1.11	−2.6	−7.1	−8.0	−16
(E_v/A) Calc.	−1.11	−2.7	−7.6	−7.7	−15
$\langle E_{\rm kin}/A\rangle$	9.6	17.1	28.7	34.4	45
$\langle v^\pi/A\rangle$	−11.2	−15.9	−28.2	−30.7	−39
$\langle v^R/A\rangle$	0.5	−3.6	−6.1	−9.7	−17
$\langle V^{2\pi}/A\rangle$	0	−0.8	−3.3	−4.6	−4.4
$\langle V^R/A\rangle$	0	0.2	1.1	2.1	3.9

The binding energies of ^{2}H, ^{3}H, ^{4}He, ^{16}O, and NM thus obtained utilizing Argonne $v(ij)$ and Urbana model VII $V(ijk)$ are listed in Table I. We note that the difference between the variational energies and experiment is rather small, particularly in comparison with the expectation values of kinetic and potential energies. From comparisons with available exact results obtained by the Faddeev and GFMC methods, the error in E_v is known to be 0, 0.1, and 0.3 MeV per nucleon in ^{2}H, ^{3}H, and ^{4}He (Wiringa, 1991). In the absence of exact results, the errors in the E_v of ^{16}O and NM are difficult to estimate, but they are likely to be ~0.5 and 1 MeV per nucleon, respectively. Thus it appears that the present Ψ_v contains the main correlations induced by the assumed interactions.

The most important correlations are generated by the $u_{t\tau}(r_{ij})S_{ij}\tau_i\cdot\tau_j$ in $U(ij)$; they are induced by the v^π and enhanced by $V^{2\pi}$. Without these the v^π and $V^{2\pi}$ give small contributions to the nuclear binding energies, and the nuclei become unbound. The $f_c(r_{ij})$ correlations are also equally important; without them the repulsive core in $v^R(ij)$ gives a large positive contribution leading to unbound nuclei. If all the other correlations were to be switched off, nuclei would still be bound. Thus one should look first for experimental information on the $f_c(r_{ij})$ and $u_{t\tau}(r_{ij})S_{ij}\tau_i\cdot\tau_j$ correlations.

The functions $f_c(r_{ij})$ and

$$f_{t\tau}(r_{ij})=u_{t\tau}(r_{ij})f_c(r_{ij}) \tag{2.8}$$

for ^{2}H, ^{4}He, ^{16}O, and NM are compared in Fig. 2. The tensor correlations $f_{t\tau}$ have little A dependence; the $r<1$ fm part of $f_c(r)$, determined principally by the repulsive

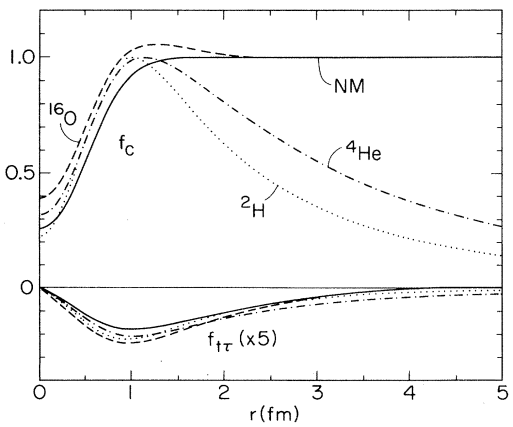

FIG. 2. The $f_c(r)$ and $f_{t\tau}(r)$ in ^{2}H, ^{4}He, ^{16}O, and NM.

core in $v^R(ij)$, is also similar in all nuclei. The differences at large r reflect mostly the different boundary conditions on $f_c(r\rightarrow\infty)$ in light ($A\leq 4$) and heavy ($A\geq 16$) nuclei. The conventional S and D components of the deuteron wave functions u_d and w_d are simply related to the u's and f_c:

$$u_d(r)=r[1-3u_\tau(r)+u_\sigma(r)-3u_{\sigma\tau}(r)]f_c(r)\ , \tag{2.9}$$

$$w_d(r)=r\sqrt{8}[u_t(r)-3u_{t\tau}(r)]f_c(r)\ . \tag{2.10}$$

The deuteron elastic-scattering form factors $A(q)$, $B(q)$, and $T_{20}(q)$ are functions of $u_d(q)$ and $w_d(q)$; the observed data are fairly explained by the u_d and w_d calculated from the Argonne model of v_{NN} (Carlson, Pandharipande, and Schiavilla, 1991).

C. Pair distribution functions

The density $\rho(\mathbf{r})$ represents the probability of finding one nucleon at $\mathbf{r}$. In a similar way the two-nucleon density $\rho_{NN}(\mathbf{r}_1,\mathbf{r}_2)$ stands for the probability of finding two nucleons simultaneously at $\mathbf{r}_1$ and $\mathbf{r}_2$. We obviously have

$$\int d^3r\,\rho(\mathbf{r})=A\ , \tag{2.11}$$

$$\int d^3r_2\rho(\mathbf{r}_1,\mathbf{r}_2)=(A-1)\rho(\mathbf{r}_1)\ , \tag{2.12}$$

$$\therefore\int d^3r_2[\rho(\mathbf{r}_1)\rho(\mathbf{r}_2)-\rho(\mathbf{r}_1,\mathbf{r}_2)]=\rho(\mathbf{r}_1)\ . \tag{2.13}$$

Generally, $\rho(\mathbf{r}_1,\mathbf{r}_2)<\rho(\mathbf{r}_1)\rho(\mathbf{r}_2)$ for $\mathbf{r}_1\sim\mathbf{r}_2$ to satisfy the above condition. The difference $\rho(\mathbf{r}_1)\rho(\mathbf{r}_2)-\rho(\mathbf{r}_1,\mathbf{r}_2)$ is often called the correlation hole, which surrounds each particle in a many-body system. The average $\bar{\rho}_{NN}(\mathbf{r}_{12})$ is defined as

$$\bar{\rho}_{NN}(\mathbf{r}_{12})=\frac{1}{A}\int d^3R_{12}\rho_{NN}(\mathbf{r}_1,\mathbf{r}_2)\ , \tag{2.14}$$

with

$$\mathbf{R}_{12}\equiv\frac{1}{2}(\mathbf{r}_1+\mathbf{r}_2)\ . \tag{2.15}$$

In NM, as well as in spherically symmetric nuclei, $\bar{\rho}_{NN}(\mathbf{r}_{12})$ is a function of $|\mathbf{r}_{12}|$, and its theoretical predictions are shown in Fig. 3 for ^{4}He, ^{16}O, and NM. The average two-proton $\bar{\rho}_{pp}(r)$ is also shown in these figures. Both $\bar{\rho}_{NN}(r)$ and $\bar{\rho}_{pp}(r)$ are sensitive to the function $f_c(r)$ and differ significantly from those obtained with Slater-determinant wave functions (Fig. 3).

We define the normalized pair distribution function $g_{\rm NM}(\rho,r)$ as

$$g_{\rm NM}(\rho,r)\equiv\bar{\rho}_{NN}(\rho,r)/\rho\ , \tag{2.16}$$

where $\bar{\rho}_{NN}(\rho,r)$ is the average two-body density in NM at density ρ. A *local-density* approximation,

$$\rho_{12}(\mathbf{r}_1,\mathbf{r}_2)\approx\rho(\mathbf{r}_1)\rho(\mathbf{r}_2)g_{\rm NM}(\sqrt{\rho(\mathbf{r}_1)\rho(\mathbf{r}_2)},r)\ , \tag{2.17}$$

is believed to be reasonable and useful (Pieper, Wiringa, and Pandharipande, 1985).

Average two-body densities associated with operators O_{ij}^p are defined as

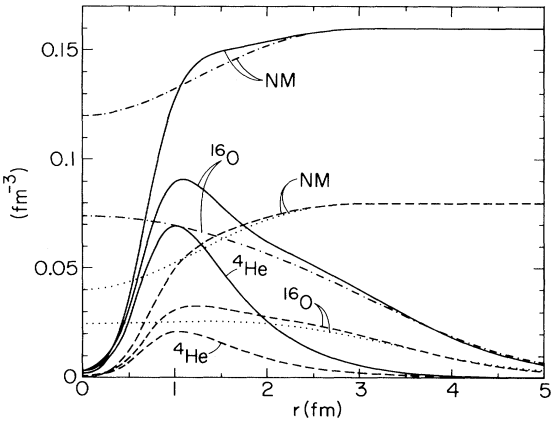

FIG. 3. The $\bar{\rho}_{NN}$ (solid lines) and $\bar{\rho}_{pp}$ (dashed lines) in ^{4}He, ^{16}O, and NM shown along with the $\bar{\rho}_{NN}$ (dot-dashed lines) and $\bar{\rho}_{pp}$ (dotted lines) obtained from the Slater determinant Φ for ^{16}O and NM.

$$\bar{\rho}_{NN,p}(r)=\frac{1}{2\pi r^2}\frac{1}{A}\sum_{i<j}\langle\Psi_0|\delta(r-|\mathbf{r}_i-\mathbf{r}_j|)O_{ij}^p|\Psi_0\rangle\ , \tag{2.18}$$

$$O_{ij}^{p=1,6}\equiv 1,\tau_i\cdot\tau_j,\sigma_i\cdot\sigma_j,\sigma_i\cdot\sigma_j\tau_i\cdot\tau_j,S_{ij},S_{ij}\tau_i\cdot\tau_j\ . \tag{2.19}$$

The $\bar{\rho}_{NN}(r)$ [Eq. (2.14)] equals $\bar{\rho}_{NN,p}(r)$ for the unit operator. These densities reveal spin-isospin correlations in the nucleus and give the expectation value of a two-body operator B:

$$B=\sum_p\sum_{i<j}B_p(r_{ij})O_{ij}^p\ , \tag{2.20}$$

$$\langle\Psi_0|B|\Psi_0\rangle=2\pi A\sum_p\int r^2dr\,B_p(r)\bar{\rho}_{NN,p}(r)\ . \tag{2.21}$$

The $\bar{\rho}_{NN,\sigma\tau}$ and $\bar{\rho}_{NN,t\tau}$ associated with operators $\sigma_i\cdot\sigma_j\tau_i\cdot\tau_j$ and $S_{ij}\tau_i\cdot\tau_j$, calculated with the variational ground state, are shown in Fig. 4. They are quite large,

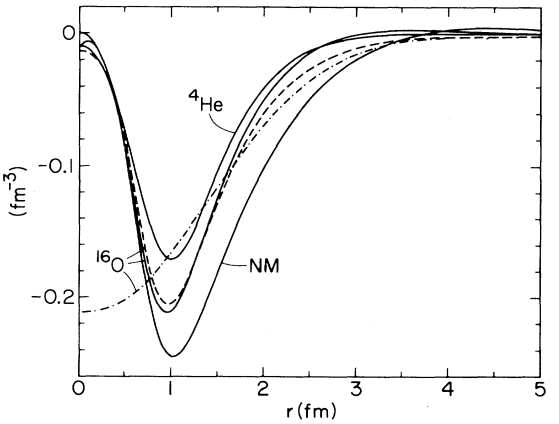

FIG. 4. The $\bar{\rho}_{NN,t\tau}$ (solid lines) for ^{4}He, ^{16}O, and NM shown along with the $\bar{\rho}_{NN,\sigma\tau}$ for ^{16}O (dashed line) and the $\bar{\rho}_{NN,\sigma\tau}$ calculated from the Φ for ^{16}O (dot-dashed line).

and hence the $\langle v^{\pi} \rangle$ is also large (Table I). The Slater determinant Φ gives $\bar{\rho}_{NN,t\tau}(r)=0$ and a large $\bar{\rho}_{NN,\sigma\tau}(r)$ due to exchange correlations, as shown in Fig. 4.

D. Momentum distribution of nucleons

The momentum distribution of nucleons in the ground state $|0\rangle$ of a nucleus is given by

$$n(\mathbf{k})=\langle 0|a_{\mathbf{k}}^{\dagger}a_{\mathbf{k}}|0\rangle \ , \tag{2.22}$$

where $a_{\mathbf{k}}$ and $a_{\mathbf{k}}^{\dagger}$ are annihilation and creation operators for a nucleon with momentum $\mathbf{k}$. Here we suppress spin-isospin indices for brevity. The $n(\mathbf{k})$ is generally calculated from the wave function Ψ_0 of the ground state:

$$n(\mathbf{k})=\frac{A}{\langle\Psi_0|\Psi_0\rangle}\int \Psi_0^{\dagger}(\mathbf{r}_1',\mathbf{r}_2,\ldots,\mathbf{r}_A)e^{i\mathbf{k}\cdot(\mathbf{r}_1'-\mathbf{r}_1)} \times\Psi_0(\mathbf{r}_1,\mathbf{r}_2,\ldots,\mathbf{r}_A) \times d^3r'\,d^3r_1\cdots d^3r_A \ . \tag{2.23}$$

Short-range correlations imply the existence of high-momentum components in the ground state, as can be clearly seen from Fig. 5 (Pieper, Wiringa, and Pandharipande, 1992), in which the $n(\mathbf{k})$ obtained by approximating the ground state Ψ_0 of ^{16}O by the Slater determinant Φ_0, the Jastrow wave function $\Psi_J=[\Pi f_c(r_{ij})]\Phi$, and the full variational wave function Ψ_v [Eq. (2.6)] are compared. We note that the $f_c(r_{ij})$ factors of Ψ_J generate a rather small fraction of $n(\mathbf{k})$ at $k>2$ fm^{-1}; most of the high-momentum distribution of nucleons stems from the tensor correlations introduced in Ψ_v.

The momentum distributions of nucleons in ^{2}H, ^{4}He, ^{16}O, and NM are compared in Fig. 6. The results for ^{2}H, ^{4}He, and ^{16}O have been obtained with the Argonne $v(ij)$ and model VII $V(ijk)$, while those for NM (Fantoni and Pandharipande, 1984) have been obtained with the Urbana $v(ij)$ with density-dependent terms that simulate the effects of $V(ijk)$. The comparison of ^{4}He with deuteron shows a significant increase in the high-momentum components; on the other hand, the $n(k\to\infty)$ of ^{4}H, ^{16}O, and NM appear to be similar.

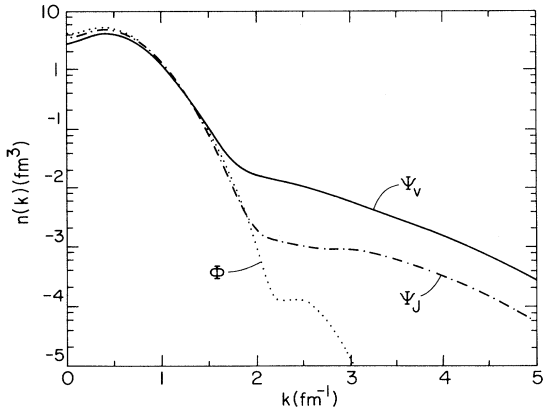

FIG. 5. Momentum distribution of nucleons in ^{16}O calculated from the full Ψ_v (solid line), Ψ_J (dot-dashed line), and Φ (dotted line).

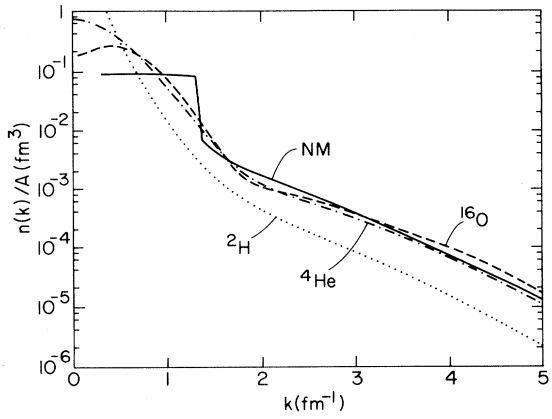

FIG. 6. The $n(k)$ per nucleon in ^{2}H, ^{4}He, ^{16}O, and NM.

E. Spectral functions

The hole-spectral function $P_h(\mathbf{k},e)$ for removing a particle of momentum $\mathbf{k}$ from the ground state $|0\rangle$ of a nucleus with A nucleons is defined as

$$P_h(\mathbf{k},e)=\sum_I |\langle I|a_{\mathbf{k}}|0\rangle|^2\delta(e+E_I-E_0) \ , \tag{2.24}$$

where $|I\rangle$ are the eigenstates of the $(A-1)$ nucleons with energies E_I. The $P_h(\mathbf{k},e)$ is regarded as the probability of finding a nucleon with momentum $\mathbf{k}$ and energy e in the nucleus, and it obeys the sum rule

$$\int P_h(\mathbf{k},e)de=n(\mathbf{k}) \ . \tag{2.25}$$

The electrons in $e,e'p$ reactions primarily interact with only one nucleon in the nucleus. The interactions of that nucleon, after it is struck by the electron, on its way out of the nucleus, are called final-state interactions (FSI). When FSI are neglected, the electron-scattering cross section is proportional to the spectral function $P_h(\mathbf{p}_m,e_m)$, where $\mathbf{p}_m=\mathbf{q}-\mathbf{p}$ is the *missing momentum*, $e_m=\omega-e_p$ is the *missing energy*, $\omega,\mathbf{q}$ are the energy momentum transferred by the electron, and $e_p,\mathbf{p}$ are those of the ejected nucleon. Hence the spectral functions are very useful in the study of electron-nucleus scattering.

The $P_h(\mathbf{k},e)$ of ^{3}He and ^{4}He have been calculated with the Faddeev (Meier-Hajduk *et al.*, 1983) and variational methods (Morita and Suzuki, 1991). It is also possible to estimate these $P_h(\mathbf{k},e)$ from the momentum distribution of nucleons, deuterons, and ^{3}H in ^{3}He and ^{4}He (Ciofi degli Atti *et al.*, 1991; Benhar and Pandharipande, 1993). The spectral functions of NM have been calculated with the Urbana $v(ij)$, with added density-dependent terms to simulate effects of $V(ijk)$, using correlated basis theory by Benhar, Fabrocini, and Fantoni (1991). Their results

are shown in Figs. 7 and 8 for $k<k_F$ and $k>k_F$. The $P_h(\mathbf{k},e)$ is sensitive to correlations in the system; for comparison, that for the uncorrelated Fermi gas (FG) is given by

$$P_h(k<k_F,e,FG)=\delta\left[e-\frac{\hbar^2}{2m}k^2\right], \tag{2.26}$$

$$P_h(k>k_F,e,FG)=0\ . \tag{2.27}$$

Correlations contribute to the $P_h(k,e)$ of NM a background term for both $k>k_F$ and $k<k_F$ which stretches over a wide range of e. The $P_h(k<k_F,e)$ has an additional quasihole peak whose width represents the lifetime of the hole. This quasihole peak becomes sharper and more distinct as k approaches k_F from below. Its strength is denoted by $Z(k)$, and Migdal (1957) has shown that in normal Fermi liquids the $Z(k\sim k_F)$ equals the magnitude of discontinuity of $n(k)$ at k_F, i.e.,

$$Z(k\sim k_F)=n(k_F-\varepsilon)-n(k_F+\varepsilon),\ \lim_{\varepsilon\to 0}\ . \tag{2.28}$$

The ground and a few low-energy excited states in nuclei like ^{3}He, ^{15}O, and ^{207}Tl can be considered as a quasihole in the doubly closed-shell nuclei ^{4}He, ^{16}O, and ^{208}Pb. They have zero width, since decay by strong interactions is not possible. Wave functions of quasihole orbitals are given by

$$\psi_{jm}(\mathbf{r}_A)=\frac{1}{\sqrt{Z_j}}\int \Psi^*_{A-1}(\mathbf{r}_1,\ldots,\mathbf{r}_{A-1}) \times\Psi_A(\mathbf{r}_1,\ldots,\mathbf{r}_A)d^3r_1\cdots d^3r_{A-1}\ , \tag{2.29}$$

where Ψ_A is the ground-state wave function of the double-closed-shell nucleus, and Ψ_{A-1} is the wave function of the $(A-1)$-nucleon quasihole state with angular momentum $(j,-m)$. The Z_j is required in order to normalize the ψ_{jm}, and it is the strength of the δ function in the spectral function $P_h(jm,e)$ of the nucleus A, calculated with quasihole operators a_{jm} instead of the plane wave

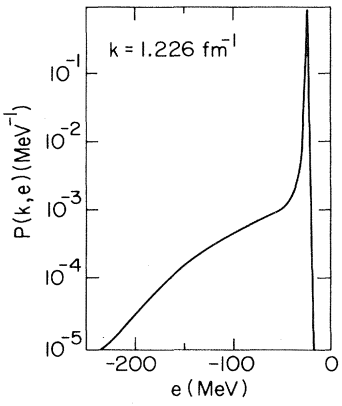

FIG. 7. Hole-spectral function for $k=1.226$ fm^{-1} in NM at equilibrium $k_F=1.33$ fm^{-1}.

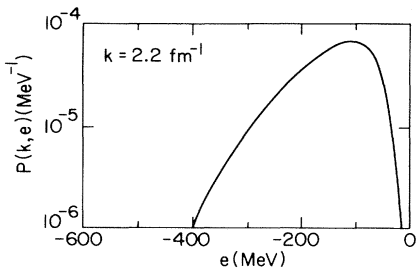

FIG. 8. Hole-spectral function for $k=2.2$ fm^{-1} in NM at equilibrium $k_F=1.33$ fm^{-1}.

$a_{\mathbf{k}}$ in Eq. (2.24).

If we approximate the nuclear wave functions by Slater determinants, as in the shell model, then the quasihole orbitals are the same as the ϕ_{jm} of the Slater determinant and $Z_j=1$. Correlations, spatial as well as spin-isospin, reduce the value of Z_j and make the quasihole orbitals ψ_{jm} more surface peaked. The ψ_{jm} of large nuclei have not been calculated with realistic nuclear interactions, but they have been estimated by Lewart, Pandharipande, and Pieper (1988) in helium liquid drops with the variational wave functions.

The normalizations Z of the $1s\,\frac{1}{2}$ state in ^{4}He and of the state with momentum k_F in NM have been studied with realistic interactions; their calculated values are $Z(1s\frac{1}{2},{}^4\text{He})=0.81$ and $Z(k_F,\text{NM})=0.71$. The surface effects in nuclei may decrease the normalization Z below its value in NM; for example, $Z(3s\frac{1}{2},{}^{208}\text{Pb})$ is estimated to be $\sim 0.6\pm 0.1$ (Pandharipande, Papanicolas, and Wambach, 1984). A measure of all the correlations in a nucleus—short range, spin-isospin, and long range—is provided by $1-Z$.

III. CORRELATION EFFECTS IN ELECTRON-NUCLEUS SCATTERING

The electrons can interact with the nucleons in various ways. At small momentum transfer the electron-nucleon interaction is essentially elastic in the electron-nucleon center-of-mass frame. The interaction via the Coulomb force is mostly with the protons, while that due to exchange of transverse photons can be with the magnetic moment of either protons or neutrons, or with the proton current. At large momentum transfers the electron-nucleon interaction becomes predominantly inelastic, leading to excited states of the nucleon and pion production. In electron-nucleus scattering experiments, the transfer of energy and momentum is carefully chosen to study different aspects of nuclear structure, and the Rosenbluth separation is used to isolate the Coulomb part.

The Coulomb interaction between a point positive charge and the electron in momentum space is given by $-e^2/q^2$. The proton, however, has a finite size, and its Coulomb interaction with the electron is given by

$-G_E^p(q,\omega)e^2/q^2$, where $G_E^p(q,\omega)$ is the proton charge form factor. The finite-size effects on the interaction of nucleon magnetic moments with the electron are similarly described by magnetic form factors $G_M^{n,p}(q,\omega)$. These form factors are empirically known from electron-nucleon scattering experiments; however, there are large uncertainties in the small neutron-electric form factor G_E^n.

A. The Coulomb sum

The cross section for the scattering of unpolarized electrons by nuclei is given in the Born approximation by the Rosenbluth formula:

$$\frac{d^2\sigma}{d\Omega d\omega}=\sigma_M\left\{\left[\frac{Q^2}{q^2}\right]^2 R_L(\mathbf{q},\omega) + \left[\frac{1}{2}\left[\frac{Q^2}{q^2}\right]+\tan^2\frac{\theta}{2}\right]R_T(\mathbf{q},\omega)\right\}, \tag{3.1}$$

where σ_M is the Mott cross section for electron-proton scattering, $Q^2=q^2-\omega^2$ is the square of the four-momentum transfer, θ is the scattering angle, and R_L and R_T are the longitudinal and transverse response functions. At $q \lesssim 600$ MeV/c, the internal excitations of the nucleon do not contribute to the longitudinal part; however, they do contribute to $R_T(\mathbf{q},\omega)$ [Bätzner *et al.* (1972)]. Thus $R_L(\mathbf{q},\omega)$ is primarily due to the Coulomb interaction between the electron and the protons and is given by

$$R_L(\mathbf{q},\omega)=\sum_I |\langle I|\rho_p(\mathbf{q})|0\rangle|^2 \times\delta(E_0+\omega-E_I)|G_E^p(q,\omega)|^2 , \tag{3.2}$$

$$\rho_p(\mathbf{q})=\sum_{i=1,A} e^{i\mathbf{q}\cdot\mathbf{r}_i}\frac{1}{2}(1+\tau_Z(i)) . \tag{3.3}$$

Here $|I\rangle$ are the eigenstates of the A nucleons with energy E_I, and $(1+\tau_z(i))/2$ is the proton projection operator. The Coulomb sum $S_L(\mathbf{q})$ is defined as

$$S_L(\mathbf{q})=\frac{1}{Z}\int_{\omega_{el}^+}^{\infty} d\omega\, R_L(\mathbf{q},\omega)/|G_E^p(q,\omega)|^2 , \tag{3.4}$$

where Z is the number of protons in the nucleus (not to be confused with the normalization factor Z). The lower limit $\omega_{\rm el}^+$ excludes the elastic electron-nucleus scattering contribution. The $S_L(\mathbf{q})$ is related to the Fourier transforms of one- and two-proton densities $\rho_p(r)$ and $\rho_{pp}(r)$ [Eq. (2.14)]:

$$S_L(\mathbf{q})=1+\rho_{pp}(\mathbf{q})-|\rho_p(\mathbf{q})|^2/Z . \tag{3.5}$$

In extended liquids the $\rho(\mathbf{q})$ vanishes for $\mathbf{q}\neq 0$, and the above equation reduces to the relation (1.1) between structure and pair distribution functions. In finite systems, like nuclei, $\rho_p(\mathbf{q})$ remains nonzero at $q\neq 0$.

Direct comparison between the theoretical $S_L(q)$ and experimental data is not possible, because the $R_L(q,\omega)$ has been measured only up to a maximum value $\omega_{\max}$. The residual integral (3.4) from $\omega_{\max}$ to ∞ is obtained from estimates of $R_L(q,\omega>\omega_{\max})$ that satisfy energy-weighted sum rules calculated theoretically. Charge-exchange nuclear interactions like the v^π [Eq. (2.2)] enhance the energy-weighted sum of $R_L(q,\omega)$ significantly above its quasifree value $q^2/2m$; its calculation is thus nontrivial. In the light nuclei a reasonable agreement between the theory (Schiavilla, Pandharipande, and Fabrocini, 1989) and experiment (Marchand *et al.*, 1985; Dow *et al.*, 1988; Dytman *et al.*, 1988) is obtained as illustrated in Fig. 9. The open circles in this figure, labeled $S_{L,\rm tr}$, show the integral of the experimental data up to $\omega_{\max}$, and the solid circles show the complete integral S_L with theoretically extrapolated $R_L(q,\omega>\omega_{\max})$. The dashed lines show values of $S_L(q)$ in ^{3}He and ^{4}He, disregarding the correlations between the two protons. Clearly the effect of correlations on the $S_L(q)$ is rather small, and best established for ^{3}He.

Equation (3.2) gives only the leading term contributing to the $R_L(\mathbf{q},\omega)$. In addition to it are small terms of order q^2/m^2 that represent relativistic corrections and two-body charge operators. These terms have been studied recently by Schiavilla, Wiringa, and Carlson, and seem to reduce the small systematic difference between the calculated and observed $S_L(q)$ for ^{3}He.

B. Nuclear transparency to protons from *e*,*e'p* reactions

When $\omega\sim q^2/2m$, the scattering can be considered as quasifree; the electron imparts momentum $\mathbf{q}$ to a single nucleon. The transparency T of a nucleus is defined as the average probability that the struck nucleon will emerge from the nucleus without colliding with other nucleons. This parameter has been measured by Garino *et al.* (1992) for protons of mean kinetic energy of 182

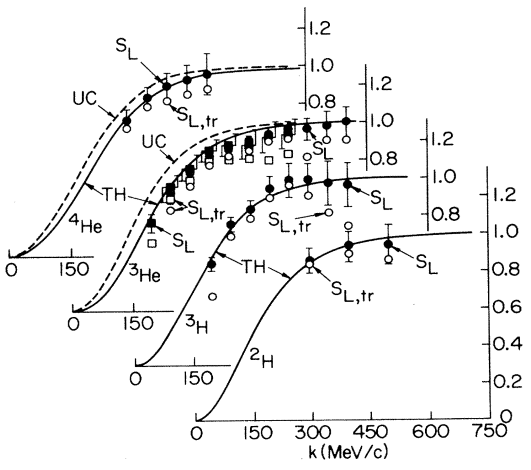

FIG. 9. Coulomb sum in ^{2}H, ^{3}H, ^{3}He, and ^{4}He.

MeV ejected from a number of nuclei. In the correlated Glauber approximation (CGA), T is given by

$$T=\frac{1}{Z}\int d^3r\,\rho_p(\mathbf{r})P_T(\mathbf{r})\ , \tag{3.6}$$

where $\rho_p(\mathbf{r})$ is the proton density, and

$$P_T(\mathbf{r})=\exp\left\{-\int_z^\infty dz'[\bar{\sigma}_{pn}(q,\rho(\mathbf{r}'))\xi_{pn}(\mathbf{r},\mathbf{r}') +\bar{\sigma}_{pp}(q,\rho(\mathbf{r}'))\xi_{pp}(\mathbf{r},\mathbf{r}')]\right\} \tag{3.7}$$

indicates the probability that a proton struck at $\mathbf{r}$ will emerge without further scattering. Here the $\hat{z}$ axis is chosen parallel to the momentum $\mathbf{q}$ of the proton, so that the x and y components of $\mathbf{r}$ and $\mathbf{r}'$ are identical. The effective pN ($N=p$ or n) scattering cross sections $\bar{\sigma}_{pN}$ depend upon q and on the density of matter at $\mathbf{r}'$, and

$$\xi_{pN}(\mathbf{r},\mathbf{r}')=\rho_{pN}(\mathbf{r},\mathbf{r}')/\rho_p(\mathbf{r})\equiv g_{pN}(\mathbf{r},\mathbf{r}')\rho_N(\mathbf{r}') \tag{3.8}$$

indicates the probability of finding a nucleon at $\mathbf{r}'$ given that there is a proton at $\mathbf{r}$. At small $|\mathbf{r}-\mathbf{r}'|$ it is appropriate to use $\xi_{pN}(\mathbf{r},\mathbf{r}')$ as defined in Eq. (3.8), since the struck proton is moving much faster than other nucleons. At large values of $|\mathbf{r}-\mathbf{r}'|$, $g_{pN}(\mathbf{r},\mathbf{r}')\sim 1$, and the approximation is inconsequential.

The transparencies calculated by Pandharipande and Pieper (1992) for 182 MeV outgoing protons are compared with the experimental data in Fig. 10. The dotted curve, showing results obtained with $g_{pN}=1$ and the observed σ_{pN} in vacuum, lies far below the data. Pauli blocking and effective-mass corrections reduce the scattering cross sections in matter significantly; the transparencies calculated with $g_{pN}=1$ and most plausible effective $\bar{\sigma}_{pN}(q,\rho(\mathbf{r}'))$, shown by the dashed line, are closer to the data. The solid curve includes correlation effects with the local-density approximation (2.17).

$$g_{pN}(\mathbf{r},\mathbf{r}')=g_{pN,NM}(\sqrt{\rho(\mathbf{r})\rho(\mathbf{r}')},|\mathbf{r}-\mathbf{r}'|)\ . \tag{3.9}$$

This g_{pN} is <1 at small $|\mathbf{r}-\mathbf{r}'|$, showing how spatial correlations increase the transparency. The present theory seems to explain the observed data quantitatively.

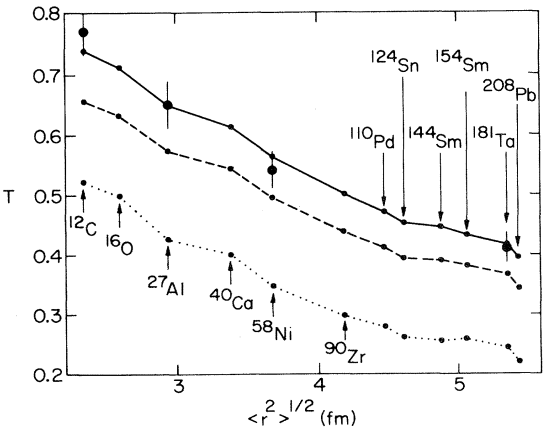

FIG. 10. Average transparency T of nuclei plotted against their rms radius. The data points are from Garino *et al.* (1992), and the theoretical curves are discussed in the text.

C. Scattering of GeV electrons by nuclei

Relativistic effects as well as internal excitations of nucleons play an important role in the scattering of GeV electrons by nuclei. The "inclusive" cross section, which includes both the Coulomb and the transverse photon-exchange interaction of the electron, is proportional to the nuclear tensor defined as

$$W^A_{\mu\nu}(\mathbf{q},\omega)=\int\frac{dt}{2\pi}e^{i(\omega+E_0)t}\langle 0|J^\dagger_\mu(\mathbf{q})e^{-iHt}J_\nu(\mathbf{q})|0\rangle\ , \tag{3.10}$$

where $J_\mu(\mathbf{q})$ are four-dimensional current operators. The tensors $W^N_{\mu\nu}(\mathbf{q},\omega)$ for free nucleons are known from experiments on protons and deuterons (Bodek and Ritchie, 1981). In the plane-wave impulse approximation (PWIA), the interaction of the struck nucleon with the residual $A-1$ nucleon system is neglected and the Hamiltonian H is approximated by $H_{A-1}+H_0$, where H_0 is the Hamiltonian of a free struck nucleon, and H_{A-1} is that of the residual system. This approximation calculates W^A from the W^N and from the spectral function $P^N_h(\mathbf{k},e)$ [Eq. (2.24)] of nucleons in nuclei:

$$W^A_{\mu\nu,IA}(\mathbf{q},\omega) =\int d\mathbf{k}\,de[ZP^p_h(\mathbf{k},e)W^p_{\mu\nu}(\mathbf{q},\omega;\mathbf{k},e) +(A-Z)P^n_h(\mathbf{k},e)W^n_{\mu\nu}(\mathbf{q},\omega;\mathbf{k},e)]\ . \tag{3.11}$$

The bound nucleons are off shell; i.e., their e^2-k^2 does not equal m^2. The W^N for $e^2-k^2\neq m^2$ has to be extrapolated from the known W^N for nucleons on the energy shell.

Once the struck hadron has scattered against a nucleon in the residual system, it is unlikely that the $J^\dagger_\mu(\mathbf{q})$ operator can revert the state to $|0\rangle$ when $\mathbf{q}$ is large. Thus it is hoped that the main effect of the final-state interactions (FSI) of the struck hadron with the residual system can be included via an attenuation factor $a(t)$; $a^2(t)$ gives the probability that the struck hadron will not have scattered by FSI up to time t. In this approximation,

$$W^A_{\mu\nu}(\mathbf{q},\omega)=\int \frac{dt}{2\pi} e^{i(\omega+E_0)t} a(t)\langle 0|J^\dagger_\mu(\mathbf{k})\exp(-i[H_{A-1}+H_0]t)J_\nu(\mathbf{k})|0\rangle$$
$$=\int d\omega' W^A_{\mu\nu,IA}(\mathbf{q},\omega')F(\omega-\omega') , \tag{3.12}$$
$$F(\omega)=Re\int_0^\infty \frac{dt}{2\pi} e^{i\omega t} a(t) . \tag{3.13}$$

This *folding function* method is similar to that used by Silver and co-workers (Silver and Sokol, 1989) to estimate the effects of FSI on the scattering of neutrons by helium liquids. We estimate $a(t)$ by approximating the interaction of the struck hadron with the residual system by an optical potential $V(\mathbf{r})$ whose real part is negligible; i.e., we take $V(\mathbf{r})$ as purely imaginary. The Glauber approximation sets

$$a(t)=\exp\left[-i\int_0^t V(\mathbf{r}_0+v\tau)d\tau\right] , \tag{3.14}$$

where $\mathbf{r}_0$ indicates the position of the struck hadron at time $t=0$, and v is its velocity. The $V(\mathbf{r})$ can be written as

$$V(\mathbf{r})=\int d^3\mathbf{r}'\xi_{NN}(\mathbf{r}_0,\mathbf{r}')W(\mathbf{r}-\mathbf{r}') , \tag{3.15}$$

where $W(r-r')$ is the imaginary part of the nucleon-nucleon interaction, and

$$\int W(\mathbf{r}-\mathbf{r}')d^3r'=\frac{i}{2}\sigma_{NN}|v| . \tag{3.16}$$

The function $W(\mathbf{r}-\mathbf{r}')$ is assumed to be a Gaussian fitted to the imaginary part of the NN scattering amplitude. At GeV energies the NN scattering is mostly inelastic and $W(\mathbf{r}-\mathbf{r}')$ has a range of ~ 0.5 fm. Equation (3.7) can be obtained from Eqs. (3.14)–(3.16) by neglecting the range of $W(\mathbf{r}-\mathbf{r}')$.

The results obtained for ^{2}H, ^{3}He, ^{4}He (Benhar and Pandharipande, 1993), and NM (Benhar, Fabrocini, and Fantoni, 1991; Benhar, Fabrocini, Fantoni, Miller, *et al.*, 1991), with PWIA and the correlated Glauber approximation (CGA) described above, are compared with the data in Figs. 11–14. Generally the data are in between the PWIA and CGA results. In ^{2}H the effects of FSI are small and the observed cross section at $\omega<\omega_{qf}$ provides a measure of the $P_h(k,e)$, or, equivalently, the momentum distribution of nucleons in the deuteron. The deep-inelastic contributions associated with nucleon excitation dominate the region at $\omega>\omega_{qf}$. At large values of q, typical in the scattering of multi-GeV electrons, relativistic kinematics gives

$$\omega_{qf}=\sqrt{q^2+m^2}-m . \tag{3.17}$$

In all nuclei other than ^{2}H, the FSI effects are significant at $\omega<\omega_{qf}$, and the data indicate their being overestimated in the CGA. It has been suggested that QCD effects reduce the interaction of the struck hadron with other nucleons below that estimated from free NN scattering, for a time called the hadronization length:

$$l_h=2\sqrt{m^2+q^2}/\Delta M^2 , \tag{3.18}$$

where $\Delta M^2\sim 0.7$ GeV^2. This *color transparency* (CT) effect causes the cross section for the scattering of the struck hadron by the other nucleons to depend upon the distance $z=|v|\tau$. Following Farrar *et al.* (1988), we set

$$\sigma_{NN}(z)=S(z)\sigma_{NN}(\text{free}) , \tag{3.19}$$
$$S(z)=\left[\frac{z}{l_h}\left[1-\frac{9\langle k_T^2\rangle}{q^2-\omega^2}\right]+\frac{9\langle k_T^2\rangle}{q^2-\omega^2}\right]\theta(l_h-z) + \theta(z-l_h) \tag{3.20}$$

with $\langle k_T^2\rangle^{1/2}=350$ MeV. This effect can be easily included in the calculation of $a(t)$ by inserting the factor $S(|v|\tau)$ in the integrand of Eq. (3.14). The results ob-

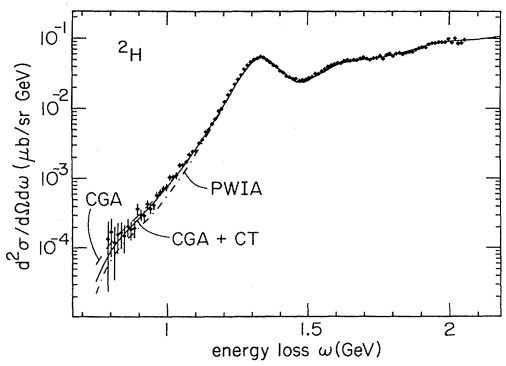

FIG. 11. Experimental (Rock *et al.*, 1982) and theoretical cross sections for the scattering of 9.79 GeV electrons by 10° from ^{2}H.

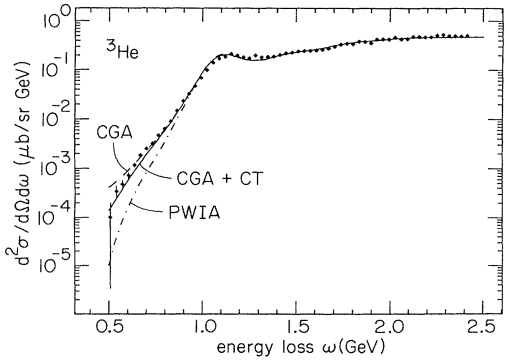

FIG. 12. Experimental (Day *et al.*, 1979) and theoretical cross sections for the scattering of 10.954 GeV electrons by 8° from ^{3}He.

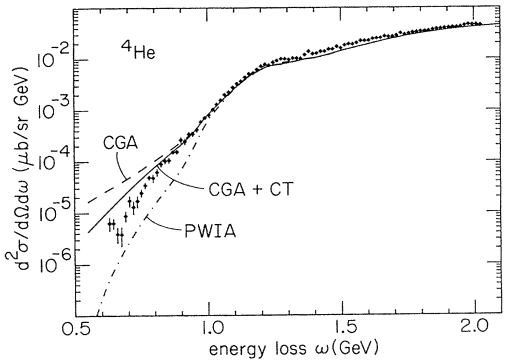

FIG. 13. Experimental (Day *et al.*, 1987) and theoretical cross sections for the scattering of 3.595 GeV electrons by 30° from ^{4}He.

tained with the CGA+CT effects seem to be in reasonable agreement with the data in Figs. 11–14, except possibly for ^{4}He.

D. Exclusive reactions

The cross sections for some inelastic electron-scattering reactions may be simply related to the normalization Z of quasiparticle states [Eq. (2.28)]. For example, the ^{207}Pb$(e,e')^{207}$Pb* reaction to low-energy quasihole states of ^{207}Pb can be considered as a single-quasihole transition. Its observed form factor $F(q)$ may be expressed, mostly through its momentum-transfer dependence, as the sum of a quenched single-particle contribution and a background term:

$$F(q)=QF_{sp}(q)+F_{bg}(q) \ . \tag{3.21}$$

The quenching factor Q is given by

$$Q=\sqrt{Z(j_i)Z(j_f)} \ , \tag{3.22}$$

where j_i and j_f are the angular momenta of the quasihole in the initial and final states (Pandharipande, Papanicolas, and Wambach, 1984). The observed transitions in ^{207}Pb and ^{208}Pb and the extracted values of $\sqrt{Z(j_i)Z(j_f)}$ are listed in Table II. It appears from this analysis that the average value of the normalization Z of low-energy quasiparticle states in ^{208}Pb is $\sim 0.6\pm 0.05$.

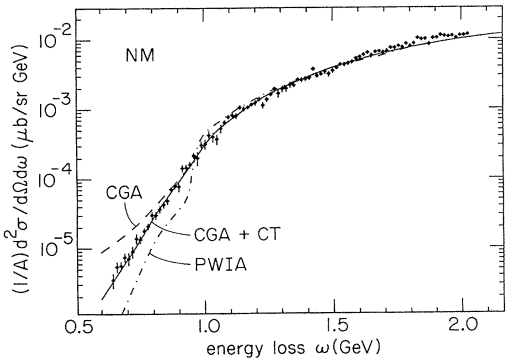

FIG. 14. Extrapolated (Day *et al.*, 1989) and calculated cross sections (per nucleon) for the scattering of 3.595 GeV electrons by 30° from NM.

TABLE II. Values of Q observed in inelastic electron scattering from ^{208}Pb and ^{207}Pb. The columns give the energy, spin, and parity of the final state and the initial and final quasiparticle orbitals. The Q values are from Heisenberg *et al.* (1982), Lichtenstadt *et al.* (1979, 1980), and Papanicolas *et al.* (1980) and have an error of ~ 0.05.

E (MeV)	J^π	j_i	j_f	Q
4.04	7^-	$2f\frac{5}{2}$	$2g\frac{9}{2}$	0.51
6.10	12^+	$1i\frac{13}{2}$	$1i\frac{11}{2}$	0.65
6.43	12^-	$1i\frac{13}{2}$	$1j\frac{15}{2}$	0.71
6.74	14^-	$1i\frac{13}{2}$	$1j\frac{15}{2}$	0.71
7.06	12^-	$1h\frac{11}{2}$	$1i\frac{13}{2}$	0.71
0.57	$5/2^-$	$2f\frac{5}{2}$	$3p\frac{1}{2}$	0.65
0.90	$3/2^-$	$3p\frac{3}{2}$	$3p\frac{1}{2}$	0.65
1.63	$13/2^+$	$1i\frac{13}{2}$	$3p\frac{1}{2}$	0.47
2.34	$7/2^-$	$2f\frac{7}{2}$	$3p\frac{1}{2}$	0.55
2.73	$9/2^+$	$3p\frac{1}{2}$	$2g\frac{9}{2}$	0.50
3.51	$11/2^+$	$3p\frac{1}{2}$	$1i\frac{11}{2}$	0.65

The cross section of the $A(e,e'p)(A-1)_h$ reaction, where A is a double-closed-shell nucleus and $(A-1)_h$ is a quasihole state, is sensitive to both the quasiparticle orbital ψ_h and $Z(h,A)$. Its PWIA cross section reads

$$d\sigma=K\sigma_{ep}|\psi_h(\mathbf{p}_m=\mathbf{p}-\mathbf{q})|^2Z(h,A) \ , \tag{3.23}$$

where K is a constant determined from the reaction kinematics, σ_{ep} is the electron-proton scattering cross section, $\mathbf{q}$ is the momentum transfer, and $\mathbf{p}$ is the momentum of the outgoing proton. The data are usually presented in the form of the reduced cross section ($d\tilde{\sigma}$):

$$d\tilde{\sigma}(\mathbf{p}_m)=d\sigma/(K\sigma_{ep}) \ . \tag{3.24}$$

The distortion of the outgoing proton wave is very significant, and in heavy nuclei the distortions of electron waves are also important. Theoretical techniques to calculate $d\tilde{\sigma}(\mathbf{p}_m)$ including effects of proton and electron wave distortions have been developed by Boffi, Giusti, and Pacati (1993). This theory can satisfactorily explain the dependence of $d\tilde{\sigma}$ on $\mathbf{p}_m$, as illustrated in Fig. 15,

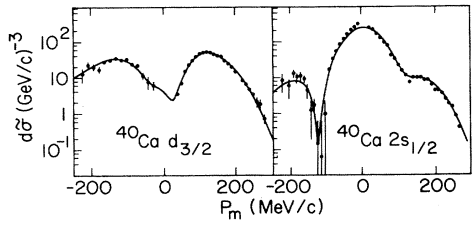

FIG. 15. Reduced cross sections $d\tilde{\sigma}(\mathbf{p}_m)$ for the ^{40}Ca$(e,e'p)^{39}$K reaction to the $1d\frac{3}{2}$ and $2s\frac{1}{2}$ quasihole states. The data are for 100 MeV outgoing protons with momenta parallel to $\mathbf{q}$ (Kramer, 1990). The results of DWIA calculations are from Lapikás (1991).

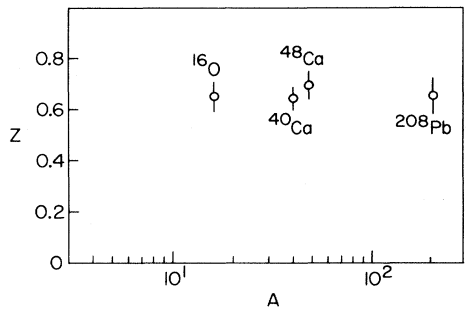

FIG. 16. Values of Z in double-closed-shell nuclei obtained from the analysis of $e,e'p$ experiments conducted at NIKHEF.

and extract values of $Z(h, A)$ from the data.

The NIKHEF group (Nationaal Instituut voor Kernfysica en Hoge-Energiefysica; van der Steenhoven and de Witt Huberts, 1991) has studied a number of $A(e,e'p)(A-1)_h$ reactions; $Z(h, A)$ values extracted from their data are shown in Fig. 16. Their average value for the Z in ^{16}O, ^{40}Ca, ^{48}Ca, and ^{208}Pb is ~ 0.65, which is consistent with that obtained from inelastic electron scattering for ^{208}Pb and ^{207}Pb.

IV. SUMMARY

The spatial correlations between nucleons in nuclei are not very strong, since the repulsive-core radius of the NN interaction (~ 0.5 fm) is much smaller than the average interparticle distance (~ 2 fm) in NM. They, accordingly, have a small effect on the Coulomb sum and on the transparency in $e,e'p$ reactions. Qualitatively an effect of the predicted magnitude is seen in the observed data, but quantitative comparisons are not yet possible. Errors in the data, and those introduced by simplifying assumptions in the analysis, implicit in the use of CGA, for example, may not be very much smaller than the correlation effect.

The tensor correlations between nucleons have a large effect on the spectral function and momentum distribution of nucleons in nuclei. The large observed cross section at $\omega < \omega_{qf}$ in the scattering of multi-GeV electrons by nuclei certainly indicates the presence of significant correlations. Final-state interaction effects are small in ^{2}H, and hence the predicted high-momentum components in the deuteron wave function seem to be confirmed by observations. On the other hand, the FSI effects are large in other nuclei.

The overall strength of correlations in nuclei, indicated by the normalization Z of quasihole states in double-closed-shell nuclei, appears to be in reasonable agreement with theory; but the effect of the nuclear surface on the Z's is large and in need of quantitative understanding.

At least two additional concerns remain in this field. First, in larger nuclei, of which ^{56}Fe is the most studied (Chen *et al.*, 1991), the Coulomb sum obtained from the observed longitudinal response is $\sim 30\%$ less than expected at $q > 300$ MeV/c. The theoretical (Schiavilla, Fabrocini, and Pandharipande, 1987) energy-weighted sums suggest that there may be only $\sim 20\%$ strength in the unobserved high-energy tail of the response, leaving $\sim 10\%$ unexplained. Second, the preliminary analysis of the recent SLAC NE18 experiment (Milner, 1993) to measure nuclear transparency for multi-GeV protons ejected in $e,e'p$ reactions has not shown the CT effect estimated by Benhar *et al.* (1992) using Eqs. (3.18)–(3.20). In the present approach the CT effect is needed to explain the observed inclusive e,e' cross sections (Figs. 12–14), suggesting that the QCD modifications of the struck nucleon's FSI may be more complex than described by Eqs. (3.18)–(3.20).

ACKNOWLEDGMENTS

It is a pleasure to thank our colleagues, J. Carlson, A. Fabrocini, S. Fantoni, C. N. Papanicolas, R. Schiavilla, I. Sick, and R. B. Wiringa, for many valuable contributions, and D. Day, S. Dytman, B. Frois, D. F. Geesaman, A. Magnon, J. P. Schiffer, and P. de Witt Huberts for illuminating discussions. This work has been supported by the U.S. National Science Foundation via Grant No. PHY89-21025 and the U.S. Department of Energy, Nuclear Physics Division, under Contract No. W-31-109-Eng-38.

REFERENCES

Aziz, R. A., V. P. S. Nain, J. S. Carley, W. L. Taylor, and G. T. McConville, 1979, J. Chem. Phys. **70**, 4430.
Bätzner, K., *et al.*, 1972, Phys. Lett. B **39**, 575.
Benhar, O., A. Fabrocini, and S. Fantoni, 1991, in *Modern Topics in Electron Scattering*, edited by B. Frois and I. Sick (World Scientific, Singapore), p. 460.
Benhar, O., A. Fabrocini, S. Fantoni, G. A. Miller, V. R. Pandharipande, and I. Sick, 1991, Phys. Rev. C **44**, 2328.
Benhar, O., A. Fabrocini, S. Fantoni, V. R. Pandharipande, and I. Sick, 1992, Phys. Rev. Lett. **69**, 881.
Benhar, O., and V. R. Pandharipande, 1993, Phys. Rev. C **47**, 2218.
Bodek, A., and J. L. Ritchie, 1981, Phys. Rev. D **23**, 1070.
Boffi, S., C. Giusti, and F. D. Pacati, 1993, Phys. Rep. **226**, 1.
Carlson, J., 1991, in *Structure of Hadrons and Hadronic Matter*, edited by O. Scholten and J. H. Koch (World Scientific, Singapore), p. 43.
Carlson, J., V. R. Pandharipande, and R. Schiavilla, 1991, in *Modern Topics in Electron Scattering*, edited by B. Frois and I. Sick (World Scientific, Singapore), p. 177.
Chen, J. P., *et al.*, 1991, Phys. Rev. Lett. **66**, 1283.
Ciofi degli Atti, C., S. Simula, L. L. Frankfurt, and M. I. Strikman, 1991, Phys. Rev. C **44**, 7.
Day, D., J. S. McCarthy, I. Sick, R. G. Arnold, B. T. Chertok, S. Rock, Z. M. Szalata, F. Martin, B. A. Mecking, and G. Tamas, 1979, Phys. Rev. Lett. **43**, 1143.
Day, D., *et al.*, 1987, Phys. Rev. Lett. **59**, 427.
Day, D., *et al.*, 1989, Phys. Rev. C **40**, 1011.
Dow, K., *et al.*, 1988, Phys. Rev. Lett. **61**, 1706.
Dytman, S., A. M. Bernstein, K. I. Blomqvist, T. J. Pavel, B. P. Quinn, R. Altemus, J. S. McCarthy, G. H. Mechtel, T. S. Ueng, and R. R. Whitney, 1988, Phys. Rev. C **38**, 800.

Fantoni, S., B. L. Friman, and V. R. Pandharipande, 1983, Nucl. Phys. A **399**, 51.
Fantoni, S., and V. R. Pandharipande, 1984, Nucl. Phys. A **427**, 473.
Farrar, G. R., H. Liu, L. L. Frankfurt, and M. I. Strikman, 1988, Phys. Rev. Lett. **61**, 686.
Friar, J. L., 1991, in *Modern Topics in Electron Scattering,* edited by B. Frois and I. Sick (World Scientific, Singapore), p. 104.
Garino, G., *et al.*, 1992, Phys. Rev. C **45**, 780.
Gibson, B. F., and B. H. J. McKellar, 1988, Few Body Syst. **3**, 143.
Hallock, R. B., 1972, Phys. Rev. A **5**, 320.
Heisenberg, J., J. Lichtenstadt, C. N. Papanicolas, and J. S. McCarthy, 1982, Phys. Rev. C **25**, 2292.
Kalos, M. H., M. A. Lee, P. A. Whitlock, and G. V. Chester, 1981, Phys. Rev. B **24**, 115.
Kramer, G. J., 1990, "The proton spectral function of ^{40}Ca and ^{48}Ca studied with the $(e,e'p)$ reaction," thesis (University of Amsterdam).
Lagaris, I. E., and V. R. Pandharipande, 1981, Nucl. Phys. A **359**, 331.
Lapikás, L., 1991, in *Proceedings of the 6th International Conference on Nuclear Reaction Mechanisms,* edited by E. Gadioli (Universita di Milano), p. 610.
Lewart, D. S., V. R. Pandharipande, and S. C. Pieper, 1988, Phys. Rev. B **37**, 4950.
Lichtenstadt, J., C. N. Papanicolas, C. P. Sargent, J. Heisenberg, and J. S. McCarthy, 1980, Phys. Rev. Lett. **44**, 858.
Lichtenstadt, J., J. Heisenberg, C. N. Papanicolas, C. P. Sargent, A. N. Courtemanche, and J. S. McCarthy, 1979, Phys. Rev. C **20**, 497.
Marchand, C., *et al.*, 1985, Phys. Lett. B **153**, 29.
Meier-Hajduk, H., Ch. Hajduk, P. U. Sauer, and W. Theis, 1983, Nucl. Phys. A **395**, 332.
Migdal, A. B., 1957, Sov. Phys. JETP **5**, 333.
Milner, R. G., 1993, private communication.
Morita, H., and T. Suzuki, 1991, Prog. Theor. Phys. **86**, 671.
Pandharipande, V. R., 1990, in *Hadrons and Hadronic Matter,* edited by D. Vautherin, F. Lenz, and J. W. Negele (Plenum, New York), p. 293.
Pandharipande, V. R., C. N. Papanicolas, and J. Wambach, 1984, Phys. Rev. Lett. **53**, 1133.
Pandharipande, V. R., and S. C. Pieper, 1992, Phys. Rev. C **45**, 791.
Papanicolas, C. N., J. Lichtenstadt, C. P. Sargent, J. Heisenberg, and J. S. McCarthy, 1980, Phys. Rev. Lett. **45**, 106.
Pieper, S. C., R. B. Wiringa, and V. R. Pandharipande, 1985, Phys. Rev. B **32**, 3341.
Pieper, S. C., R. B. Wiringa, and V. R. Pandharipande, 1992, Phys. Rev. C **46**, 1741.
Rock, S., R. G. Arnold, P. Bosted, B. T. Chertok, B. A. Mecking, I. Schmidt, Z. M. Szalata, R. C. York, and R. Zdarko, 1982, Phys. Rev. Lett. **49**, 1139.
Schiavilla, R., A. Fabrocini, and V. R. Pandharipande, 1987, Nucl. Phys. A **473**, 290.
Schiavilla, R., V. R. Pandharipande, and A. Fabrocini, 1989, Phys. Rev. C **40**, 1484.
Schiavilla, R., V. R. Pandharipande, and R. B. Wiringa, 1986, Nucl. Phys. A **449**, 219.
Silver, R. N., and P. E. Sokol, 1989, *Momentum Distributions* (Plenum, New York).
Stoks, V., R. Timmermans, and J. J. de Swart, 1992, Institute of Theoretical Physics, University of Nijmegen, Report THEF-NYM-92.05.
Svensson, E. C., V. F. Sears, A. B. D. Woods, and P. Martel, 1980, Phys. Rev. B **21**, 3638.
van der Steenhoven, G., and P. K. A. de Witt Huberts, 1991, in *Modern Topics in Electron Scattering,* edited by B. Frois and I. Sick (World Scientific, Singapore), p. 510.
Wiringa, R. B., 1991, Phys. Rev. C **43**, 1585.
Wiringa, R. B., 1993, Rev. Mod. Phys. **65**, 231.
Wiringa, R. B., V. Fiks, and A. Fabrocini, 1988, Phys. Rev. C **38**, 1010.
Wiringa, R. B., R. A. Smith, and T. L. Ainsworth, 1984, Phys. Rev. C **19**, 1207.